# Effect of nanoparticles on streamer propagation and breakdown of vegetable oil-pressboard interface in non-uniform electric field

Cite as: AIP Advances **8**, 085211 (2018); https://doi.org/10.1063/1.5043591
Submitted: 11 June 2018 • Accepted: 04 August 2018 • Published Online: 13 August 2018

Wei Yao, Zhengyong Huang, Jian Li, et al.

# Effect of nanoparticles on streamer propagation and breakdown of vegetable oil-pressboard interface in non-uniform electric field

Wei Yao, Zhengyong Huang,[a] Jian Li,[a] Gang Chen, Jianfeng He, and Jawad Ahmad
*State Key Laboratory of Power Transmission Equipment & System Security and New Technology, School of Electrical Engineering, Chongqing University, China*

(Received 11 June 2018; accepted 4 August 2018; published online 13 August 2018)

Electrical equipment is always subjected to various of operating conduction and voltage waves which cause insulation failure on the surface of pressboard (PB). In this paper, pre-breakdown streamers of surface discharge on the interface of PB in vegetable oil based $Fe_3O_4$ nanofluids (NFs) were observed by the shadowgraph method under lightning impulse voltage. The images indicate that streamers of NFs impregnated PB show more branches than that of pure oil impregnated PB. The stopping length of streamers propagation is calculated by shadowgraph images for NFs and pure oil. Results suggest that the stopping length of NFs impregnated PB is shorter under the same extra voltage. Secondary reverse streamer is generated at the dissipation process by the reverse electric field, which is caused by residual space charge imparted by primary streamer. Results indicate that the $Fe_3O_4$ nanoparticles have reduced the length of secondary reverse streamer. The positive and negative lightning breakdown voltage of $Fe_3O_4$ NFs impregnated PB is increased by 24% and 12% at 50mm gap, respectively. In addition, nanoparticles have effectively changed the electric field distribution resulting in the alleviation of streamer concentrated along the parallel direction of PB, and increased the lightning impulse breakdown voltage. 
https://doi.org/10.1063/1.5043591

## I. INTRODUCTION

Insulation oil, which is an insulation and cooling medium, is an important part of power transformer insulation systems. Traditionally, mineral oil is widely used in power transformers due to their excellent electrical characteristics. However, mineral insulating oil being derived from the petroleum products, is a non-renewable resource and it is thought to be hazardous to the environment. Recently, vegetable insulating oil, which is an environmentally friendly and high flash point (+300 °C) liquid dielectric, has drawn attention as a potential industrial substitution to traditional mineral oil for power transformers.[1–4] The physical, chemical, electrical properties of vegetable oil have met the requirements of the insulating oil used for transformers. Being a mature insulation technology, oil-paper insulation has been widely used in the power equipment.[5] Vegetable oil is more conducive in retarding the aging of paper insulation, which is mainly due to the higher saturated solubility in water, absorbing water in paper in the process of aging.[6,7] Thus, the oil–paper insulation system of vegetable insulating oil has better anti-aging properties than mineral oil.

Nanofluids (NFs), which are formed by adding nanoscale particles to the base fluid, offer notable advantages in enhancing insulation properties.[8–11] Nanoparticles could enhance the breakdown voltage of insulating oil due to its capability to generate carrier trapping and capture free electrons.[12]

[a]Corresponding author: Zhengyong Huang (e-mail: huangzhengyong@cqu.edu.cn) and Jian Li (e-mail: lijian@cqu.edu.cn)

 

Improving the insulating properties of insulating oil and providing a long-term sustainable operation of power transformer. Meng Hung et al. reported that the addition of a certain amount of $TiO_2$ nanoparticles to mineral oil impregnated PB result in the enhancement of AC and positive lightning impulse voltage by 12.2% and 32%, respectively.[13] Jun Liu et al. studied the effect of $TiO_2$ nanoparticles on dielectric frequency response properties of oil-paper composite insulation. Results showed that the nanoparticles have enhanced the AC breakdown voltage of oil by 30% in addition to enhancement in the real and imaginary part of the complex permittivity of oil-paper composite insulation.[14] The liquid dielectric produces a weak discharge channel under the action of local high field strength and a "treelike" shape is generated in a very short time under external energy injection.[15–18] Recently, the streamer initiation and propagation in mineral oil based NFs at the pre-breakdown stage of discharge process have been reported.[19–23] The results showed that the nanoparticles are able to hinder the streamer propagation due to the electrons trapping and reduce mobility of negative charges. However, fewer works exist on study focusing on the effect of nanoparticles on the streamer propagation and dissipation of surface discharge in vegetable oil impregnated PB, therefore, it is necessary to capture the surface discharge images by shadowgraph method in order to examine the mechanism behind it.

In this paper, the shadowgraph imaging method is utilized to analyze the effect of $Fe_3O_4$ nanoparticles on the streamers propagation and dissipation stages of pre-breakdown in vegetable oil impregnated PB recorded at 25mm insulating gap under lightning impulse voltage. The breakdown voltage and time are tested in order to analyze the effect of nanoparticle on surface discharge of oil impregnated PB. The relative dielectric constant of vegetable oil, PB and nanoparticles which caused the interface charge is analyzed using streamer images of NFs impregnated PB.

## II. EXPERIMENTATION

### A. Preparation of nanoparticles, NFs and NFs impregnated PB

The NFs have prepared by two-step method. Firstly, Ferroferric oxide ($Fe_3O_4$) nanoparticles were prepared by high temperature decomposition method.[24] At first, 3.24 g of iron (III) chloride hexahydrate, 11 g sodium-oleate-vigorous mixture, 25 ml ethanol and 42 ml of n-hexane were taken in a beaker and stirred for 6 hours under constant temperature of 60 °C in water bath. The resultant mixture were then washed three times with deionized water, 1.1 g iron oleate precursor and 5 ml octadecene mixed in 0.32 ml oleic acids were added with stirring at 800r/min and heating process at 200 °C for 2 hours which was further continued to 320 °C for 48 hours. Secondly, it was cooled to room temperature and subsequently centrifuged for 3000r and washed with ethanol and cyclohexane several times.

In order to prepare NFs, nanoparticles with mass fraction of 0.01% were dispersed by ultrasonic dispersion method into a type of vegetable insulating oil, the FR3 mechanized from the Cargill. After that, the NFs and the FR3 were dried at 85 °C in vacuum chamber for 72 h.

The PB, mechanized from the Weidmann, has a thickness of 2 mm. Before impregnation in NFs, the PB was dried first in a vacuum chamber at 90 °C for 48 h in order to keep the moisture content of each paper specimen below 0.5 wt.%. Finally, the PBs were impregnated in dried NFs and pure oil in vacuum box at 85 °C for 48 h.

### B. High-voltage experiment and test electrode

The lightning impulse breakdown voltage test device is shown in Figure 1, which illustrates the development pattern of the NFs impregnated PB. The entire system consists of three parts: the test cell, the impulse generator and measurement component, and the discharge recording equipment. The lightning impulse breakdown, which is a key parameter for insulation evaluation of dielectric liquids, was measured in accordance with the IEC 60897 standard. A three stage impulse generator was used to provide the lightning impulse with maximum voltage up to 900 kV for an energy of 33.74 kJ. This impulse generator was used to deliver a standard lightning impulse of 1.2 (±30%)/50 μs (±20%) and a switching impulse of 250 (±20%)/2500 μs (±60%). The voltage waveform was measured by a high-voltage capacitive resistor voltage divider and recorded with the help of an oscilloscope

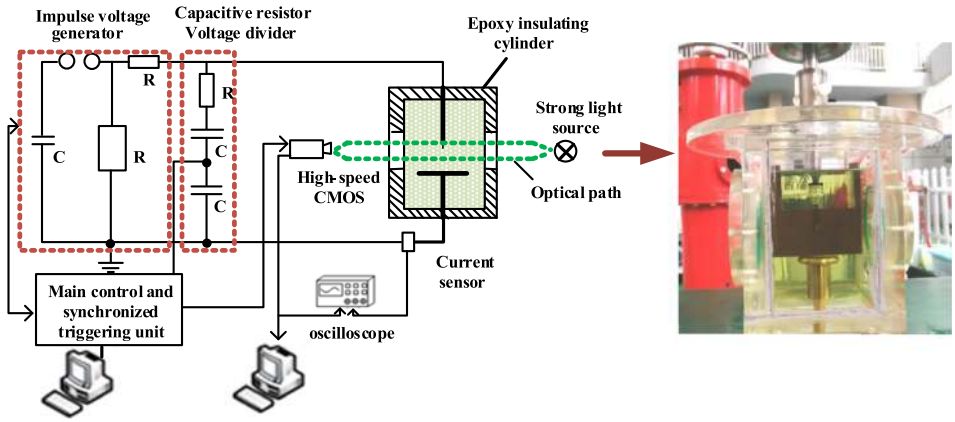


FIG. 1. Principle diagram of test system for discharge in NFs impregnated PB.

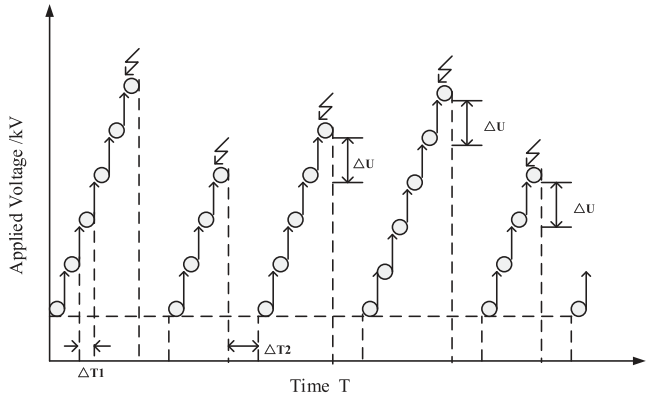


FIG. 2. Rising-voltage method.

(LeCroy WaveRunner 610zi). The sampling rate was 10 GS/sand the bandwidth was 1 GHz. The high-voltage electrode served as the needle electrode and ground electrode is plate electrode. The radius of curvature of tungsten needle is 50 μm ± 5 μm, and the diameter of plate electrode is 20 cm. The gap distance of the electrodes was adjustable to maximum 60 mm.

### C. Experimental procedure

In this paper, the rising-voltage method is used, which can be performed under both impulse and AC conditions.[25] For a single test, the applied voltage should be increased from an initial voltage level at a constant rate till the breakdown occurs. Repeat the single test procedure after a resting interval, until a significant number of breakdown voltages are obtained. It is widely and successfully used in AC breakdown tests due to the ease control of voltage increasing process. However for impulse tests, the voltage can only be increased shot by shot or step by step.

According to IEC 60897, standards for lightning breakdown tests of insulating liquid, adopt the rising-voltage method. As shown in Figure 2, ΔT1 is the time interval between two consecutive shots; ΔT2 is the time interval between two consecutive tests and ΔU (3kV) is voltage of step increment.

## III. RESULTS AND DISCUSSIONS

### A. Structural characterization

The transmission electron microscopy (TEM) images of the $Fe_3O_4$ nanoparticles are presented in Figure 3a. It can be seen that the shape of nanoparticles is mostly spherical and the diameter is small

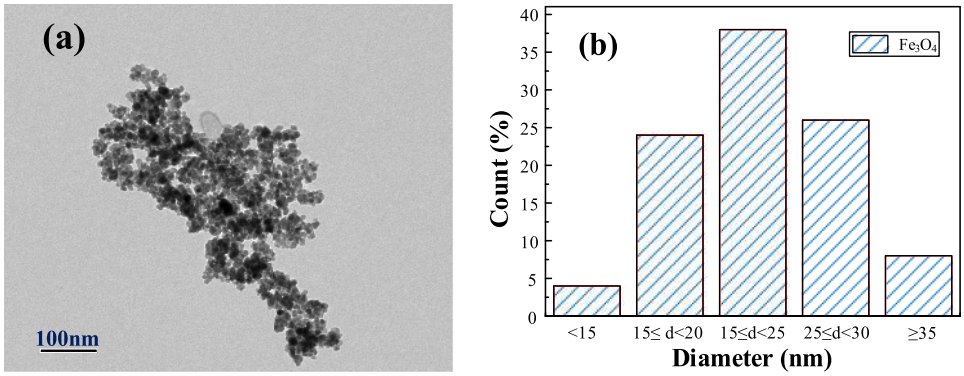


FIG. 3. High resolution TEM images of $Fe_3O_4$ nanoparticles (a) and diameter statistical analysis result with 500 nanoparticles (b).

dispersion. Statistical analysis of 500 $Fe_3O_4$ nanoparticles of TEM images (Figure 3b) reveals that the diameter of $Fe_3O_4$ nanoparticles are about 15~25 nm obtained using high temperature decomposition method.

### B. Streamer shape under same lightning voltage

Figure 4 shows the streamer shadow photographs of the oils impregnated PB under 60 kV negative lightning impulse voltage at 25 mm gap, and the shape of streamer is thin filamentous branches. The positive steamer is propagated along with PB with many branches in oil. The streamer of NFs impregnated PB has more branches and shows shorter shopping length ($Fe_3O_4$ NFs~13.5 mm, pure oil~18.3 mm) than that of pure oil.

Figure 5 shows the streamer shadow photographs of the oils impregnated PB under 75 kV negative lightning impulse voltage at 25 mm gap. The treelike streamers of samples develop along the PN direction to ground electrode. In the pure vegetable oil impregnated PB, the streamer near the needle tip and the head is of shrubby shape, and the streamer in middle of oil shows few branches. Compared to pure oil impregnated PB, the head of streamers in NFs impregnated PB is longer, and the middle of streamers with more branches. Under the same applied voltage of 75 kV, the stopping length of streamers in $Fe_3O_4$ NFs is 13.2 mm, which is shorter than that of the pure oil (~16.7mm).

### C. Streamer propagation and dissipation

Since, the shape of positive streamer is filamentary, and the propagation of positive streamer is not obvious by shadowgraph method. This paper only analysed the difference between the pure oil and NFs impregnated PB for negative streamer propagation and dissipation. Figure 6 shows the shadowgraph images of negative streamer propagation and dissipation for two samples. According to the images of FR3 under 81 kV voltage, the shape of streamer is shrub like near the needle at 10 μs and begins to propagate towards PB. At 20 μs, the main channel of streamer starts to propagate fast along the PB with few oil branches. At 30 μs, the shrub shape of streamer near the needle starts to disappear gradually, however, the head of streamer with lateral branch continues to propagate along

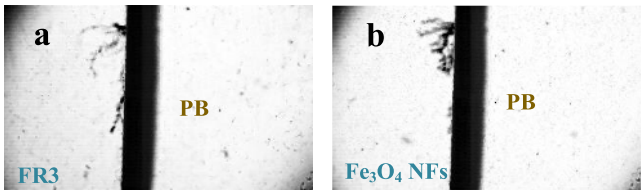


FIG. 4. The streamer shape of oil-paper under 60kV positive lightning impulse voltage.

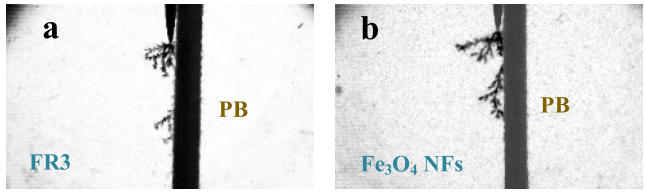


FIG. 5. The streamer shape of oil-paper under 75 kV negative lightning impulse voltage.

the PB in the direction of the ground electrode, and the streamer is developed to stopping length (figure 6c of FR3). At 40 μs, the whole streamer is gradually dissipated.

Compared with pure oil, the branches of streamer in NFs impregnated PB have increased significantly. According to the images of NFs impregnated PB under 90 kV applied voltage, the streamer shape near the needle is similar to pure oil at 10 μs, and exhibits the shrub shape. However, at 20 μs, the shape of streamer in NFs is different as compared to pure oil. The streamer in NFs propagates along the PB with more branches compared with pure oil. There exists a number of long branches located at the head of streamer which propagate in the oil. The streamer develops to shopping length at 30 μs and then begins to dissipate. Since, the applied voltage of two samples are close to breakdown voltage, the stopping length of streamers are close to the oil gap.

According to the shadow imaging of streamers and current signal, the needle electrode also shows a secondary streamer and a positive current at 100~200 μs. Figure 7 shows the secondary streamer images that remove the previous streamer of samples and the voltage and current signal of $Fe_3O_4$ NFs impregnated PB. The length of secondary reverse streamer in NFs is shorter than that of pure oil. The local ionization, thermal gasification and space charge in liquid dielectric may lead to the initiation and propagation of streamer. The secondary streamer maybe generated by the reverse electric field, which is caused by the residual space charge resulting from primary streamer and called the secondary reverse streamer.[26,27] The dissipation process of primary streamer is gradually decreased due to the external electric field at the tip of the needle electrode. Therefore, the reverse electric field is greater than the external electric field and secondary reverse streamer starts to appear.

### D. Stopping length

Figure 8 shows the relationship between the positive and negative voltage and its stopping length under the 25 mm oil gap for two oil samples. Under positive lightning voltage, all oil samples show a stopping length about 5 mm at initial stage and the maximum stopping length of 20 mm is recorded when the voltage is close to the breakdown voltage. Under the same external lightning voltage, the length of pure oil is longer than that of NFs. Under negative lightning voltage, the stopping length is similar to that of positive at the initial stage which is about 5 mm for all samples.

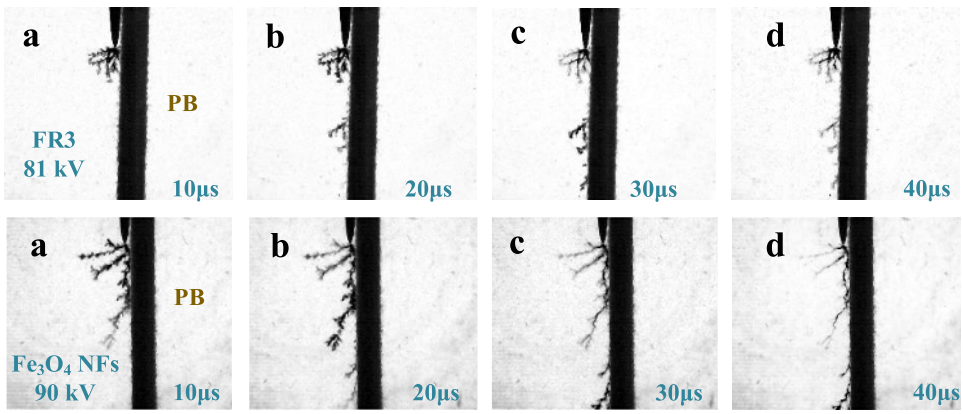


FIG. 6. The streamer propagation of NFs impregnated pressboard under negative lightning impulse voltage.

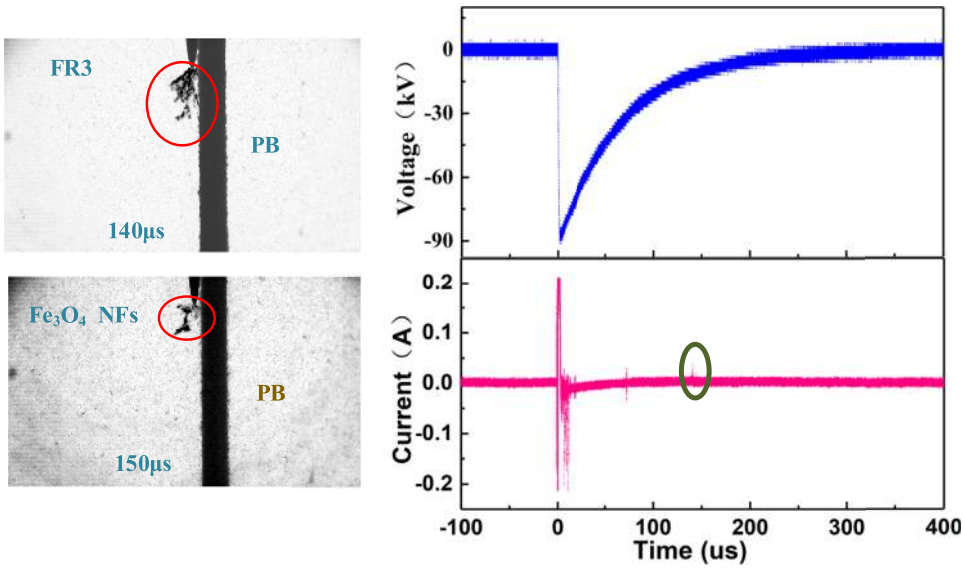


FIG. 7. The images of secondary reverse streamer for NFs impregnated PB (left) and voltage/current signal of $Fe_3O_4$ NFs impregnated PB.

However, the maximum shopping length of NFs impregnated PB is closer to the oil gap 25mm length ($Fe_3O_4$ NFs~22.5mm, pure oil~19.1 mm). It is indicated that the NFs impregnated PB needs a higher breakdown voltage per unit length as compared to pure oil impregnated PB under both positive and negative lightning voltage, and nanoparticles can inhibit the development of the streamer resulting in the increase of breakdown voltage. The initial discharge ionization occurs mostly in the concentrated position of the electric field on the interface of dielectric.[28,29] However, the electric field strength located in the interface between insulating oil and PB is more concentrated under the applied voltage.[30,31] Therefore, the initial discharge occurs and develops along the surface of the PB, which eventually leads to the surface discharge.

## E. Breakdown voltage

The results of positive and negative lightning breakdown voltage of oil samples under different gap are shown in Figure 9. It can be seen that the nanoparticles have enhanced the breakdown voltage of vegetable oil impregnated PB. The positive lightning breakdown voltage of $Fe_3O_4$ NFs impregnated PB has increased by 37% and 24% recorded at 15mm and 50mm gaps respectively. On the other hand, the negative lightning breakdown voltage of the $Fe_3O_4$ NFs impregnated PB is increased by

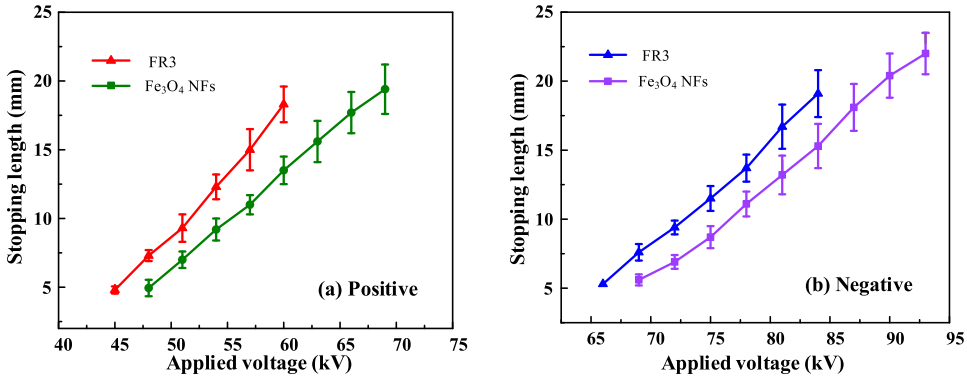


FIG. 8. Stopping length of streamer at various voltage at 25 mm oil gap. (a): positive; (b) negative.

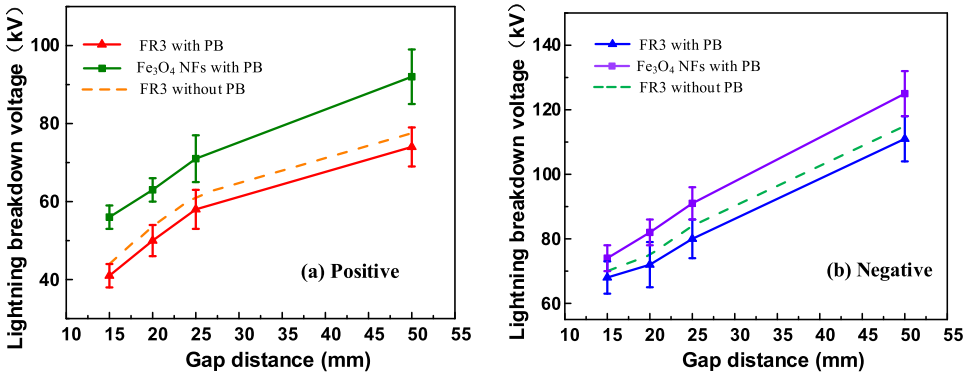


FIG. 9. Breakdown voltage under lightning impulse at different oil gap.

13% at 50 mm gap. The amplitude of positive lightning impulse breakdown is greater than the negative breakdown voltage, and the space charge theory for NFs without PB has also explained this phenomenon.[19] Nanoparticles can generate charge carrier trapping and capture the migrated electrons resulting in negative ions,[32] thus change the distribution of electric fields in gap, especially weaken the positive electric field in middle of oil gap which consequently, result in the enhancement of positive breakdown voltage. In addition, the lightning breakdown voltage of vegetable insulating oil without PB at different gap are measured, and the results confirming the literature data in small gaps under non-uniform electric field.[33] It is indicated that the PB almost has no effect on the breakdown voltage in vegetable insulating oil under small gaps.

Figure 10 shows the relationship between the different oil gap of samples and the breakdown velocity, which is calculated from the gap distance and lightning breakdown time. It indicates that the nanoparticles have decreased the breakdown velocity of vegetable oil impregnated PB. The positive lightning breakdown velocity of $Fe_3O_4$ NFs impregnated PB is 1.16 km/s at 25mm gap, which is decreased by 14% as compared to pure oil impregnated PB. Similarly, the negative lightning breakdown velocity of $Fe_3O_4$ NFs impregnated PB is decreased by 15% as compared of pure oil. The results indicate that the nanoparticles effectively decrease the breakdown velocity and retard the development of streamers in NFs impregnated PB. The streamer velocity less than 1km/s ($d \leqslant 20$mm) is generally classified in the $1^{th}$ mode of propagation. The streamer velocity between 1 km/s and 5km/s ($20 < d \leqslant 50$mm) are generally classified in the $2^{th}$ mode of propagation.[34,35] The $3^{th}$ mode streamers can be appeared in vegetable insulating oil at acceleration voltage for small electrode gap.[36–38] The fast $4^{th}$ model streamer with a velocity > 10 km/s of vegetable insulating oil at the beginning of propagation occurs above +100 kV, compared to +160 kV in mineral oil.[39] In addition, the average streamer propagation velocities in mineral oil are generally lower than that of vegetable insulating oil under same values of testing voltages.[34,40] The nanoparticles can reduce

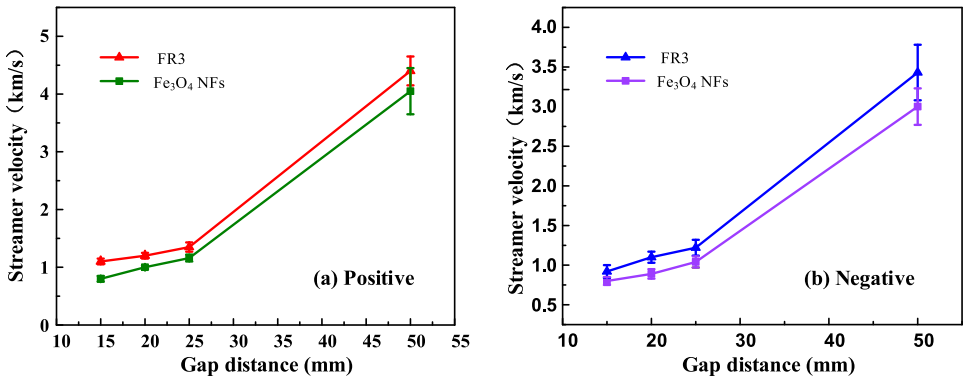


FIG. 10. Breakdown velocity under lightning impulse voltage at different oil gap.

the velocity of streamer development and enhance the breakdown voltage of vegetable insulating oil-pressboard interface.

### F. Effect of nanoparticles on streamer propagation

The NFs impregnated PB consists of three kinds of dielectrics, including vegetable oil, nanoparticles and PB. According to the breakdown theory of composite dielectric, the electric field distribution inside dielectric is determined by the conductivity of the dielectric under the effect of a constant DC electric field. However, under the lightning impulse voltage, due to the short time, the field distribution is determined by the relative permittivity of each dielectric.[41]

For pure oil impregnated PB, the relative dielectric constants of vegetable oil and PB at room temperature are 3.08 and 4.1, respectively. According to the gauss law and connection conditions at the medium interface, the interface charge $\sigma$ between oil and PB can be expressed as follows:

$$\boldsymbol{e}_n \cdot \left(\boldsymbol{D}_{pb} - \boldsymbol{D}_{oil}\right) = \sigma \tag{1}$$

where $\boldsymbol{e}_n$ is the interface unit normal vector, $\boldsymbol{D}_{pb}$ and $\boldsymbol{D}_{oil}$ is electric displacement vectors in PB and vegetable oil, respectively. As the relative dielectric constant of vegetable oil and PB is different, the interfacial charge is also expressed as:

$$\begin{cases} \varepsilon_{pb}E'_{pb} - \varepsilon_{oil}E'_{oil} = \delta \\ \varepsilon_{pb}E''_{pb} - \varepsilon_{oil}E''_{oil} = 0 \end{cases} \tag{2}$$

where the $E'_{pb}$, $E''_{pb}$, $E'_{oil}$ and $E''_{oil}$ is the electric field of the PB and oil in vertical and parallel PB direction, respectively. As the relative dielectric constant of the PB is greater than that of vegetable oil, the larger electrical field result in the direction parallel to PB. The electric field force of the interface charge will direct the free charge in the oil to move along the direction of the PB in the discharge process, that is, the streamer develops along the direction of the PB. On the contrary, if the relative dielectric constant of oil is greater than that of the PB, the charge of the PB-oil interface will produce the repulsion to the charge in the oil, thus making the streamer develop into the oil.

In the NFs impregnated PB insulation system, the relative dielectric constant of nanoparticles $Fe_3O_4$ is 80, which is larger than that of vegetable oil. The interface charge of nanoparticles-oil is:

$$\begin{cases} \varepsilon_{np}E'_{np} - \varepsilon_{oil}E'_{oil} = \delta \\ \varepsilon_{np}E''_{np} - \varepsilon_{oil}E''_{oil} = 0 \end{cases} \tag{3}$$

where the $E'_{np}$ and $E'_{np}$ arethe electrical field of nanoparticles in vertical and parallel direction, respectively. $\varepsilon_{np}$ is relative dielectric constant of the nanoparticles. As the relative dielectric constant of the nanoparticles is greater than that vegetable oil, the electric field force generated by interface charge will attract the charge in the oil. Therefore, the propagation of streamer in NFs impregnated PB will result in more branches development in the oil than that of pure oil as shown in figure 11.

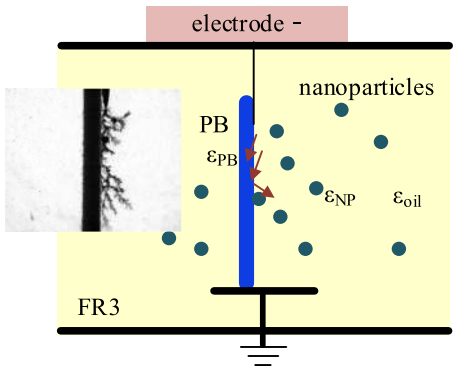


FIG. 11. A schematic diagram of electric field distribution in NFs impregnated PB.

In the NFs impregnated PB, assumed that there exists a point charge $q$ in the oil, with distance to the PB and a nanoparticle taken as $d_1$ and $d_2$, respectively. Then, the force $F_1$ by PB-oil interface charge to point charge and $F_2$ nanoparticles-oil interface charge to point charge can be expressed as follows:

$$\begin{cases} F_1 = \dfrac{q \cdot q_1'}{4\pi\varepsilon_0(2d_1)^2}\vec{e} \\ F_2 = \dfrac{q \cdot q_2'}{4\pi\varepsilon_0(2d_2)^2}\vec{e} \end{cases} \tag{4}$$

where $\varepsilon_0$ is the vacuum permittivity, $q_1'$ is the equivalent mirror charge at the PB internal of distance $d_1$, $q_2'$ is the equivalent mirror charge of inside nanoparticle of distance $d_2$, and $\vec{e}$ is the unit direction vector of the vertical PB, $q_1'$ and $q_2'$ can be expressed by

$$\begin{cases} q_1' = q\dfrac{\varepsilon_{oil} - \varepsilon_{pb}}{\varepsilon_{oil} + \varepsilon_{pb}} \\ q_2' = q\dfrac{\varepsilon_{oil} - \varepsilon_{np}}{\varepsilon_{oil} + \varepsilon_{np}} \end{cases} \tag{5}$$

Assuming that NFs impregnated PB contains $n$ nanoparticles, the total force $F$ of point charge $q$ in the oil is:

$$F = F_1 - F_2 - F_3 - \cdots - F_{n+1} \tag{6}$$

Comprehensive (4) ~ (6), $F$ can be also expressed as:

$$F = \frac{q^2(\varepsilon_{\text{oil}} - \varepsilon_{\text{pb}})}{16\pi\varepsilon_0 d_1^2(\varepsilon_{oil} + \varepsilon_{pb})}\vec{e} - \frac{q^2(\varepsilon_{\text{oil}} - \varepsilon_{np})}{16\pi\varepsilon_0 d_2^2(\varepsilon_{oil} + \varepsilon_{np})}\vec{e} - \cdots \tag{7}$$

According to the equation 7, it can be seen that the charge is only affected by the interface charge of the PB in pure oil impregnated PB. Since, $\varepsilon_{oil} < \varepsilon_{pb}$, the charge force in the oil gets reversed to the inside of the PB, that is, the charge in the oil is attracted by interface charge. The direction of streamer development is along the direction of the PB. For NFs impregnated PB, the interface charge by nanoparticles-oil makes the charge in the oil to move around the nanoparticles, reducing the attraction by that of PB, which leads to a large number of lateral branches developed in the oil in discharge process. In addition, the number of collateral branches is related to the nanoparticles concentration. Therefore, NFs impregnated PB effectively alleviates the streamer concentrated along the parallel direction of PB, and lightning impulse breakdown voltage is increased.

## IV. CONCLUSION

In this research, vegetable oil based $Fe_3O_4$ nanoparticles was prepared and impregnated with pressboard. From shadowgraph imaging results, streamers of nanofluids impregnated pressboard develop more branches in nanofluids and the stopping length are shorter in the propagation process as compared to pure oil impregnated pressboard. Secondary reverse streamer is generated in the dissipation process by the reverse electric field, which is mainly caused by residual space charge imparted by primary streamer. The positive lightning breakdown voltage of $Fe_3O_4$ nanofluids impregnated pressboard is increased by 24% under 50mm gap. Similarly, the negative lightning breakdown voltage is enhanced by 13% under 50 mm gap. The positive and negative lightning breakdown velocity of $Fe_3O_4$ nanofluids impregnated pressboard gets decreased by 14% and 15% compared to pure oil impregnated pressboard, respectively. The mechanism is that the interface charge located in nanoparticles-oil interface makes the charge in the oil to moves around the nanoparticles, reducing the attraction by that of pressboard, which leads to a large number of lateral branches developed in the oil in discharge process. Therefore, nanofluids impregnated pressboard effectively alleviates the streamer concentrated along the parallel direction of pressboard, and the lightning impulse breakdown voltage is increased.

## ACKNOWLEDGMENTS

The authors acknowledge National Natural Science Foundation of China (Grant No. 51425702), the 111 Project of the Ministry of Education, China (B08036) and the national key basic research program of China (973 program) (No. 2015CB251003).

[1] S. S. Kumar, M. W. Iruthayarajan, M. Bakrutheen, and S. G. Kannan, IEEE Transactions on Dielectrics & Electrical Insulation **23**, 2068 (2016).
[2] H. M. Wilhelm, M. B. C. Stocco, L. Tulio, W. Uhren, and S. G. Batista, IEEE Transactions on Dielectrics & Electrical Insulation **20**, 1395 (2013).
[3] K. Bandara, C. Ekanayake, T. Saha, and H. Ma, Energies **9**, 258 (2016).
[4] M. Alam, D. Akram, E. Sharmin, F. Zafar, and S. Ahmad, Arabian Journal of Chemistry **7**, 469 (2014).
[5] T. K. Saha and P. Purkait, Journal of Chemical Physics **11**, 144 (2015).
[6] G. K. Frimpong, T. V. Oommen, and R. Asano, IEEE Electrical Insulation Magazine **27**, 36 (2011).
[7] L. Yang, R. Liao, C. Sun, J. Yin, and M. Zhu, in Influence of vegetable oil on the thermal aging rate of kraft paper and its mechanism, 2010, p. 381.
[8] D. E. A. Mansour, A. M. Elsaeed, and M. A. Izzularab, IEEE Transactions on Dielectrics & Electrical Insulation **23**, 3364 (2017).
[9] H. Jin, T. Andritsch, I. Tsekmes, R. Kochetov, P. Morshuis, and J. Smit, IEEE Transactions on Dielectrics & Electrical Insulation **21**, 1100 (2014).
[10] Y. Lvorcid, M. Rafiq, C. Li, and B. Shan, Energies **10**, 1025 (2017).
[11] G. D. Peppas, A. Bakandritsos, V. P. Charalampakos, E. C. Pyrgioti, J. Tucek, R. Zboril, and I. F. Gonos, ACS Applied Materials & Interfaces **8**, 25202 (2016).
[12] Y. Du, Y. Lv, C. Li, M. Chen, J. Zhou, X. Li, Y. Zhou, and Y. Tu, Journal of Applied Physics **110**, 619 (2011).
[13] M. Huang, L. Wang, Y. Ge, Y. Z. Lv, B. Qi, and C. R. Li, AIP Advances **8**, 035205 (2018).
[14] J. Liu, L. Zhou, G. Wu, Y. Zhao, L. Ping, and P. Qian, Proceedings of the CSEE **19**, 510 (2011).
[15] Q. Liu and Z. D. Wang, IEEE Transactions on Dielectrics & Electrical Insulation **18**, 285 (2011).
[16] O. Lesaint, Journal of Physics D Applied Physics **49**, 144001 (2016).
[17] P. Rozga, IEEE Transactions on Dielectrics & Electrical Insulation **18**, 720 (2011).
[18] A. Beroual, M. Zahn, A. Badent, and K. Kist, IEEE Electrical Insulation Magazine **14**, 6 (1998).
[19] J. G. Hwang, M. Zahn, F. M. O'Sullivan, L. A. A. Pettersson, O. Hjortstam, and R. Liu, Journal of Applied Physics **107**, 416 (2010).
[20] Y. Zhou, S. Sui, J. Li, Z. Ouyang, Y. Lv, C. Li, and W. Lu, Journal of Physics D Applied Physics **51** (2018).
[21] J. G. Hwang, F. O'Sullivan, M. Zahn, and O. Hjortstam, in Modeling of Streamer Propagation in Transformer Oil-Based Nanofluids, 2008, p. 361.
[22] Y. Lv, Y. Ge, Q. Du, Q. Sun, B. Shan, M. Huang, C. Li, B. Qi, and J. Yuan, IEEE Transactions on Plasma Science **45**, 1704 (2017).
[23] Y. Lv, Q. Wang, Y. Zhou, C. Li, Y. Ge, and B. Qi, AIP Advances **6**, 231 (2016).
[24] J. Li, B. Du, F. Wang, W. Yao, and S. Yao, Physics Letters A **380**, 604 (2016).
[25] W. Hauschild and W. Mosch, IEE Power **324** (1992).
[26] Q. Liu and Z. Wang, in Phenomenon of secondary reverse streamer in an ester transformer liquid under lightning impulse voltage, 2013, p. 955.
[27] Q. Liu and Z. D. Wang, Journal of Physics D Applied Physics **44**, 405203 (2011).
[28] J. F. Kolb, R. P. Joshi, S. Xiao, and K. H. Schoenbach, Journal of Physics D Applied Physics **41**, 3850 (2008).
[29] D. Ariza, M. Becerra, R. Hollertz, L. Wågberg, and C. Pitois, IEEE Transactions on Dielectrics & Electrical Insulation **24**, 2371 (2017).
[30] J. Dai, Z. D. Wang, and P. Jarman, Dielectrics & Electrical Insulation IEEE Transactions on **17**, 1327 (2010).
[31] Q. Liu, Z. D. Wang, P. Dyer, and D. Walker, in Accumulative effect on streamer propagation of lightning impulses on oil/pressboard interface, 2011, p. 1.
[32] J. Li, Z. Zhang, P. Zou, B. Du, and R. Liao, Modern Physics Letters B **26**, 1250095 (2012).
[33] P. Rozga and M. Stanek, IEEE Transactions on Dielectrics & Electrical Insulation **24**, 991 (2017).
[34] O. Lesaint and G. Massala, IEEE Transactions on Dielectrics & Electrical Insulation **5**, 360 (2002).
[35] O. Lesaint and M. Jung, Journal of Physics D Applied Physics **33**, 1360 (2000).
[36] P. Rozga, IEEE Transactions on Dielectrics & Electrical Insulation **22**, 2754 (2015).
[37] P. Rozga, Bulletin of the Polish Academy of Sciences Technical Sciences **64**, 171 (2016).
[38] M. Unge, S. Singha, S. Ingebrigtsen, D. Linhjell, and L. E. Lundgaard, in Influence of molecular additives on positive streamer propagation in ester liquids, 2014, p. 1.
[39] C. T. Duy, O. Lesaint, A. Denat, and N. Bonifaci, IEEE Transactions on Dielectrics & Electrical Insulation **16**, 1582 (2009).
[40] P. Rozga, Energies **9**, 467 (2016).
[41] J. Jadidian, M. Zahn, N. Lavesson, O. Widlund, and K. Borg, Applied Physics Letters **100**, 172903 (2012).